CCDTL section for Linac4

G. De Michele[1], F. Gerigk[1] M. Pasini[1], M. Vretenar[1], A. Tribendis[2]

1) CERN, Geneva, Switzerland
2) BINP, Novosibirsk, Russia

Abstract

For the new Linac4 injector at CERN a Cell Coupled Drift Tube Linac (CCDTL) has been designed for the energy range between 50 and 100MeV. We report here the final design and the procedures used for the generation of the geometry parameters of the machine. Two prototype cavities have been produced and a summary of the low and high power test is reported. A revised mechanical design of the structure is also presented.

Introduction

For the new Linac4 injector at CERN a Cell Coupled Drift Tube Linac (CCDTL) has been designed for the energy range between 50 and 100 MeV. This structure is basically composed by several 3-gaps Alvarez structures (accelerating cells, AC) coupled together by a small coupling cavity (coupling cell, CC) located at the equator of the accelerating cells (Figure 1)[1]. A set of 3 accelerating cells and 2 coupling cells forms a "module" which will be fed by a single klystron. The CCDTL section consists of 21 accelerating cavities grouped in 7 modules. Each accelerating cavity houses 2 drift-tubes and three gaps. Two full-scale prototypes of the CCDTL structures have been produced to validate the technology of the construction and successfully tested at high power [2]. With respect of the old layout [3], this new design makes use of an increased shunt impedance to allow a more uniform accelerating gradient throughout the section. The CCDTL cavity prototypes have been built and tested. Results are reported in [2] and a summary is given here. The up-to-date layout is based on the results of such prototypes in terms of maximum accelerating gradient, Q-value and peak-field.

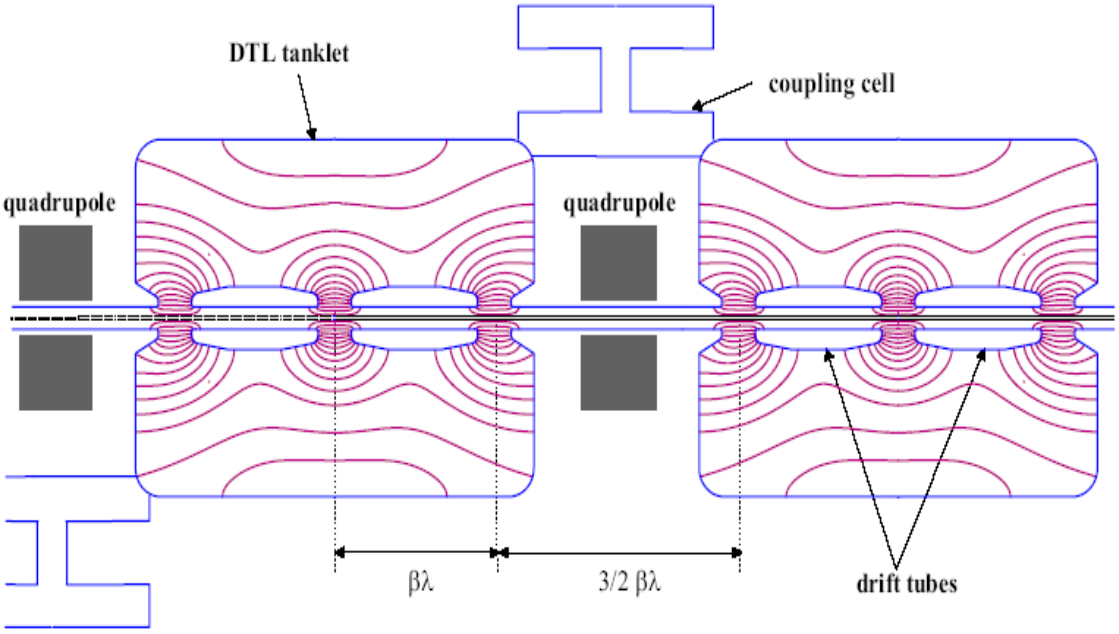

Figure 1 CCDTL scheme.

Geometry description

As mentioned above the accelerating cell is basically a small Alvarez structure where the distance between the gaps is constant. When the synchronous particle travels through such a structure, it will experience a small phase slip since the particle velocity will match the synchronous velocity only in 1 gap. The main parameter to define is hence the so called geometric β (β_g) which defines the distance between two adjacent accelerating gaps.
This parameter changes as a function of the energy of the incoming beam and details on how to determine correctly this parameter will be given in the next section. All other geometric details are chosen in order to maximize the shunt impedance and at the same time to have a maximum Kilpatrick factor (Kp) of 1.7 (high power test demonstrated that a value of Kp=1.8 was reached within few days of conditioning). The solution of the Maxwell equations is done by means of the tuning program CDTfish which allows to set the geometry parameters as

shown in Figure 2. More details on the geometry are shown in Figure 3, Figure 4. In Table 1 the geometric variables and constants for the optimized shunt impedance are given.

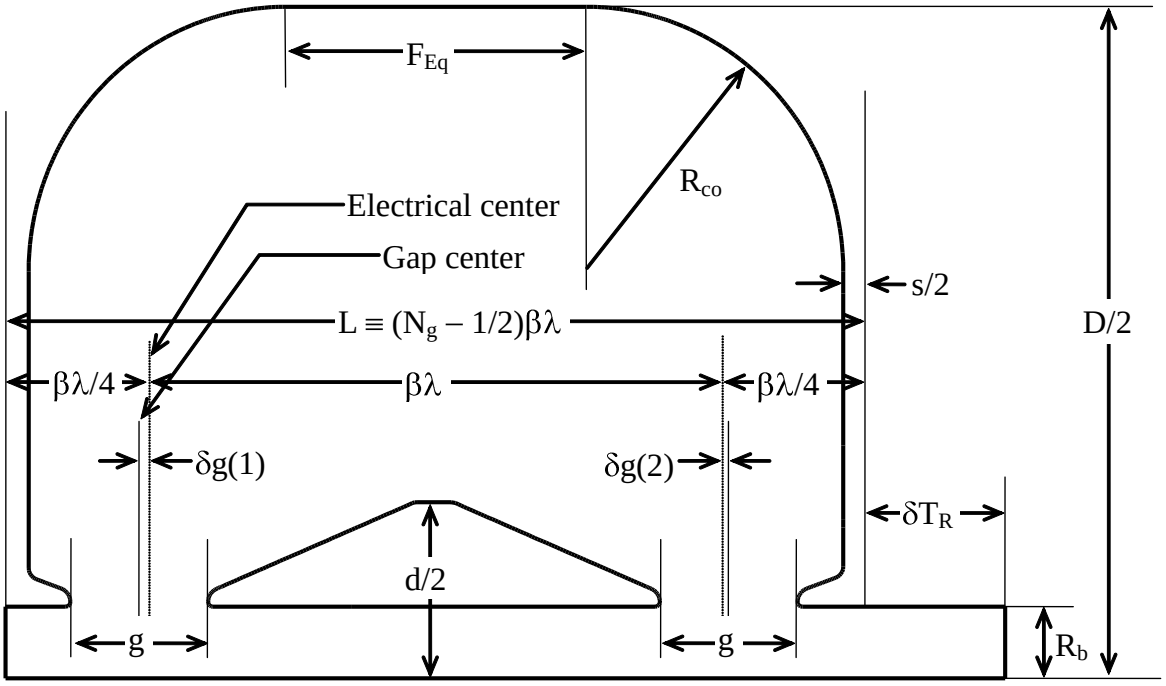

Figure 2 Full cavity of a one-drift-tube, 2-gap CCDTL.

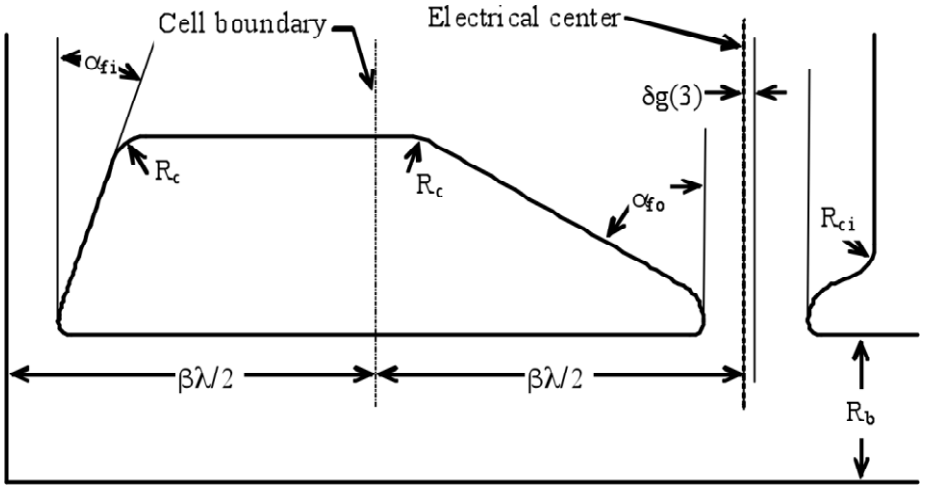

Figure 3 Details near the drift tube in a CCDTL cavity.

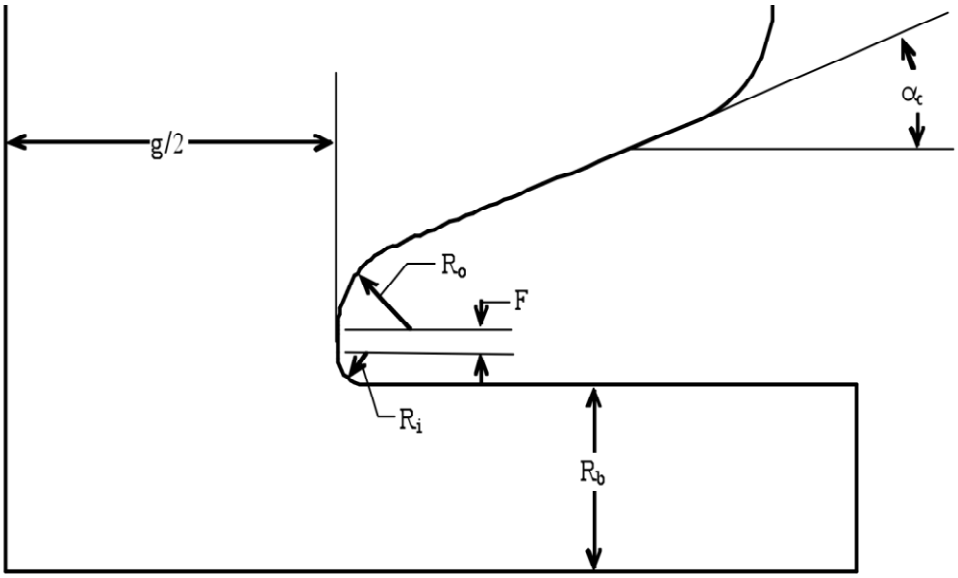

Figure 4 Detail near the nose in a CCDTL cell.

Control-file name	Geometric name	Value [cm]
BETA	β	variable
DIAMeter	D	52
GAP_Length	g	variable
EQUATOR_flat	F_{Eq}	variable
INNER_CORNer_radius	R_{ci}	1.5
OUTER_NOSE_radius	R_o	0.7
INNER_NOSE_radius	R_i	0.2
FLAT_length	F	0.3
CONE_angle	α_c	20*
SEPTUM_thickness	s	variable
BORE_radius	R_b	1.4
LEFT_BEAM_tube	δT_L	8
RIGHT_BEAM_tube	δT_R	8
DT_DIAMeter	d	9.5
DT_CORNer_radius	R_c	0.25
DT_OUTER_NOSE_radius	R_{do}	1.2
DT_INNER_NOSE_radius	R_{di}	0.2
DT_FLAT_length	F_d	0.3
DT_STEM_Diameter	d_{Stem}	2.4
DT_FACE_angle	α_f	0.0
DT_OUTER_FACE_angle	α_{fo}	75*
DT_INNER_FACE_angle	α_{fi}	75*

* degree

Table 1 Geometric parameters nomenclature.

Layout generation

The tool utilized for the generation of the CCDTL section is based on an EXCEL spreadsheet, which has been reported in the Appendix B. The layout has been generated assuming the incoming beam energy to be equal to 50 MeV. The main limits on the value for the accelerating gradient are:

1. Power available at the module equal to 1MW
2. Kilpatrick factor less then 1.7

For the first point, the total power used by a module is calculated by adding the dissipated power of each cavity as calculated by Superfish increased by 20% margin and the beam loading for 40 mA current. Once a voltage and a distance between gaps are given, only the initial phase is chosen in order to have -20 deg synchronous phase in the center gap. For the first cavity it is also necessary to choose the so-called SEPTUM_thickness parameter. We find that with the choice of the first SEPTUM_thickness equal to 2cm allows us to have a smooth increase of the effective shunt impedance along the structure.
The structure of the datasheet is based on very few free parameters, namely the geometric beta, the gradient and the phase of the first gap of each accelerating cavity. Practically, one chooses the accelerating gradient and the geometric beta β_g in order to maximize the transit time factor. The geometric beta is a characteristic of a cavity related to the distance between the RF gaps. It refers to the velocity of particle that is synchronous with the RF fields in that section of the cavity. The phase is calculated in order to match the design synchronous phase at the center of the cavity (middle of the second gap).
The initial beam parameters for the evaluation of the layout are shown in Table 2.

Particle	H^-	
Initial Energy	50.0	MeV
Mass	939.294	MeV/c^2
Frequency	352.2	MHz
Initial β	0.3139	#
Current	40.0	mA

Table 2 Initial beam parameters.

For each cell in the cavity, the voltage, the transit time factor, the particle phase, the energy gain per gap, the total energy per gap and the beta particle at the end of the gap are calculated starting from a parameterization of the SUPERFISH simulations. The layout can be recursively fill in once all the values in the first cavity are calculated. Once the geometry of the drift tube and the geometric beta are chosen, the equator flat is given by the following formula:

$$Eq\_flat = \frac{5}{2}\beta_g \cdot \lambda + septum - 2R_{co}$$

where R_{co} is the outer corner radius of the cavity and it is a constant equal to 4cm.
The septum is chosen equal to 2cm in the first cavity in order to have a more uniform geometry in the following cavities. For the other cavities it can be calculated by the following formula:

$$Septum = \beta_{endg3,1CAV} \cdot \lambda \left(\frac{3}{2} + \frac{\Delta\varphi}{360} \right) - L_{cc} - \frac{septum}{2} - \beta_{g,1CAV} \cdot \lambda - \beta_{g,2CAV} \cdot \lambda$$

with $\Delta\varphi = \varphi_{gap1,2CAV} - \varphi_{gap3,1CAV}$

where $\varphi_{gap3,1CAV}$ is the phase in the third cell of the previous cavity and $\varphi_{gap1,2CAV}$ is the phase in the first cell in the next cavity.
The geometric beta is a fundamental parameter for the calculation of the layout which allows maximizing the transit time factor for the three gaps. This corresponds to minimizing the phase shift from the synchronous phase in each gap. The phase shift $\Delta\phi$ can be calculated in accordance with the following formula (valid also for the relativistic case):

$$\Delta\phi = 360 \cdot \frac{\Delta T}{T} \cdot \frac{1-\beta^2}{\beta^2}$$

In the worst case (i.e. at lower energy) one has 1.6 degrees phase shift, which means a transit time factor difference $\frac{\Delta T}{T} \cong 5 \times 10^{-4}$.

RF Simulations

2D Simulations

Initial simulations were performed in order to maximize the shunt impedance by changing the cavity diameter, constant for the whole CCDTL section in order to simplify the geometry [3]. The effective shunt impedance decreases rapidly with the particle velocity. This is the reason why around 100MeV Linac4 has adopted a π-mode structure (PIMS).
The constant diameter does not compromise the efficiency of the design because can be found a diameter which is still in the optimum range for all particle velocities. The optimum diameter was at about 51.5 cm and after reviewing the mechanical constraints for the insertion of the quadrupole it has been decided to use a slightly larger diameter of 52 cm. Similarly all other geometric parameters were analyzed and full parameterization of the RF properties of the cavity was determined as a function of the geometric β and accelerating gradient.
The power to be provided for each module by the klystrons is shown in Table 3. The effective shunt impedance per unity length (ZTT) to be expected on all CCDTL modules and the Q-value are listed in the Table4. The normalized length for ZTT is $L = \frac{5}{2}\beta_g \cdot \lambda + septum$. The power values are multiplied by 1.2 to account for additional losses with respect to simulations. The losses on end walls, stems and coupling slots have been taken into account. Consistently the ZTT and Q-values are multiplied by a factor 1/1.2.

N. Module #	Dissipated power [kW]	beam load [kW]	tot power* [kW]
1	450	266	806
2	488	283	868
3	529	298	934
4	575	313	1003
5	575	314	1004
6	575	313	1003
7	576	312	1003

*(dissipated power*1.2)+(beam load)

Table 3 Total power to be provided by the klystrons.

N. Cavity #	ZTT [MΩ/m]	ZTT* [MΩ/m]	Q-value #	Q-value* #
1	55	46	48264	40220
2	55	46	48489	40407
3	55	45	48708	40590
4	54	45	48897	40748
5	54	45	49078	40898
6	53	45	49230	41025
7	53	44	49379	41149
8	52	44	49509	41258
9	52	43	49619	41349
10	51	43	49726	41438
11	51	42	49805	41504
12	50	42	49895	41579
13	49	41	49946	41622
14	49	40	50025	41688
15	48	40	50052	41710
16	47	39	50113	41761
17	47	39	50116	41763
18	46	38	50171	41809
19	45	38	50167	41806
20	44	37	50214	41845
21	44	36	50178	41815

*83% of nominal value to take into account additional losses with respect to the simulations

Table 4 Effective shunt impedance per unity length and Q-value for CCDTL structure.

3D Simulations

For the 3D RF design of the CCDTL the CST MWS® suite has been used. The coupling coefficient has been calculated at different energy: 50MeV, 75MeV, 102MeV. The stop-band has been closed by tuning the coupling cell. In Table 5 one can see the coupling coefficient *k* for different energy and the relative stop-band. The Figure 5 shows the 3D design from CST MWS®.

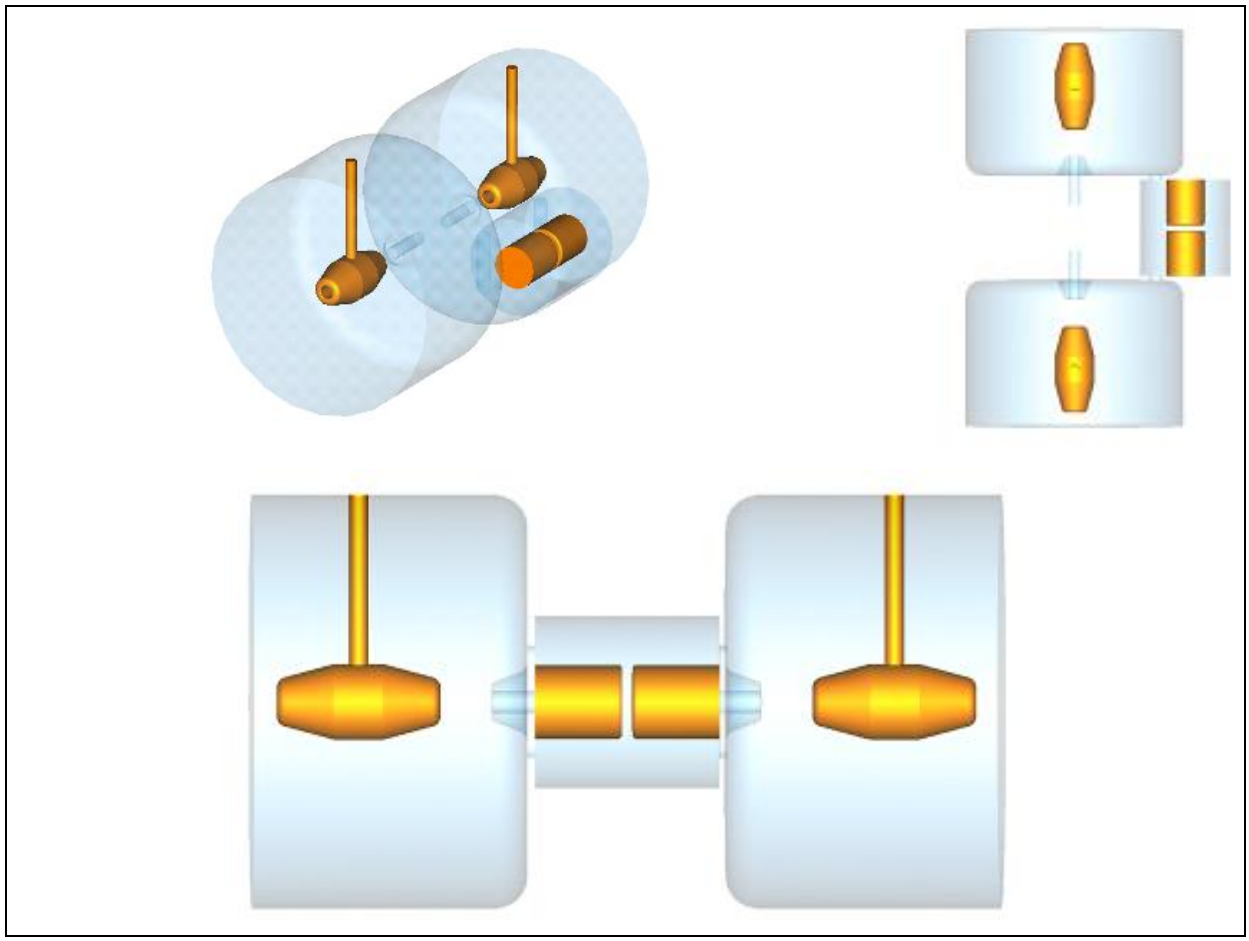

Figure 5 CCDTL 3D design.

Energy [MeV]	k [%]
50	0.83
75	0.70
102	0.59

Table 5 Simulated coupling coefficient at different energies.

CCDTL circuit model analysis

The modeling of a single module has been performed by means of PSpice code. The analysis looks after the field error introduced by frequency errors of each resonant cavity. These errors can be classified in two types: the first one is derived by residual tuning errors and can be considered as static error; the second one comes from, for example, the change of the external temperature or variation of the cooling water temperature or flow. This latter type we refer to as dynamic error. Figure 6 shows a schematic of the module lumped circuit. The circuit parameters have been determinated numerically with the Superfish/MWS codes and are reported in Table 6.

	L	Q
AC	175.67*2e-9	47400
CC	19.37*2e-9	12500

Table 6 Circuit parameters.

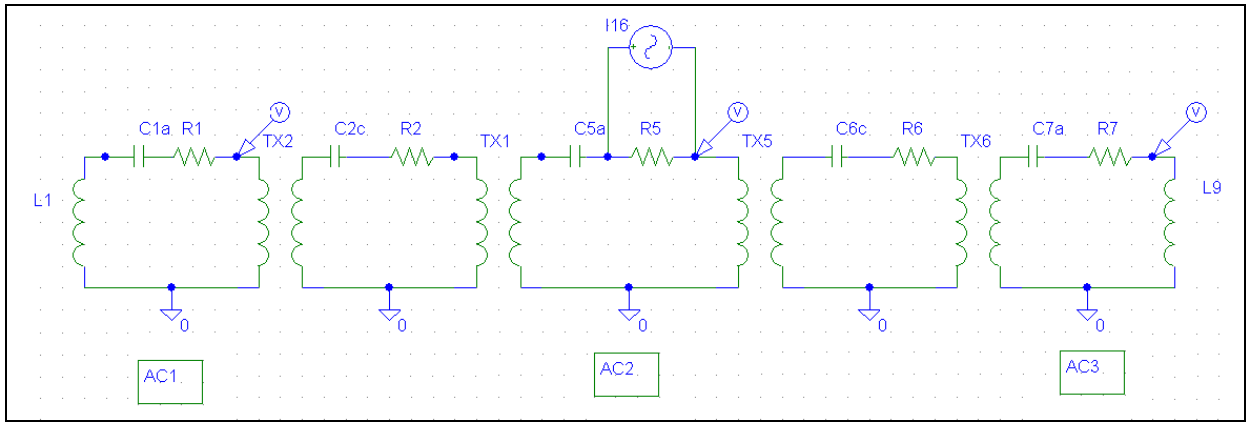

Figure 6 Schematic of the module.

Static error

We consider here the worst case of the CCDTL section, i.e. the last module where the coupling coefficient k=0.0059. We assume a residual frequency error of ±20kHz in the cavities distributed as indicated in Table 7. These distributions will include the maximum field error.

		AC1	CC1	AC2	CC2	AC3	T.S. [%/MHz]
Case 1	Frequency [MHz] Error	352.18 -20kHz	352.18 -20kHz	352.20 0kHz	352.22 +20kHz	352.22 +20kHz	0.69
Case 2	Frequency [MHz] Error	352.18 -20kHz	352.20 0kHz	352.20 0kHz	352.20 0kHz	352.22 +20kHz	5.63
Case 3	Frequency [MHz] Error	352.18 -20kHz	352.19 -10kHz	352.20 0kHz	352.21 +10kHz	352.22 +20kHz	3.17
Case 4	Frequency [MHz] Error	352.22 +20kHz	352.22 +20kHz	352.20 0 kHz	352.22 +20 kHz	352.22 +20 kHz	4.99
Case 5	Frequency [MHz] Error	352.22 +20kHz	352.20 0 kHz	352.20 0 kHz	352.20 0 kHz	352.22 +20 kHz	6.59
Case 6	Frequency [MHz] Error	352.22 +20kHz	352.21 +10 kHz	352.20 0 kHz	352.21 +10 kHz	352.22 +20 kHz	5.77
Case 7	Frequency [MHz] Error	352.18 -20 kHz	352.22 +20 kHz	352.20 0 kHz	352.18 -20 kHz	352.22 +20 kHz	10.55
Case 8	Frequency [MHz] Error	352.18 -20 kHz	352.21 +10 kHz	352.20 0 kHz	352.19 -10 kHz	352.22 +20 kHz	8.10
Case 9	Frequency [MHz] Error	352.20 0kHz	352.18 -20kHz	352.20 0kHz	352.22 +20kHz	352.20 0kHz	5.86
Case 10	Frequency [MHz] Error	352.20 0kHz	352.19 -10kHz	352.20 0kHz	352.21 +10kHz	352.20 0kHz	5.86

Table 7 Frequency errors distribution.

The tilt sensitivity (T.S.) of the voltage respect to the average voltage has been calculated for each case. In the worst case (Case 7) we get 10.55%/MHz and the maximum field error for ±20kHz is then 0.2%.

Dynamic error

The frequency variation due to the temperature variation $\Delta T=10K$ is estimated to be lower than 50kHz. This variation is applied to both accelerating and coupling cells. In order to bring back the working mode to 352.2MHz one chooses to insert a tuner in the AC in the middle of the module. The tuner frequency variation necessary to match the correct resonant frequency of the $\pi/2$-mode is equal to 150kHz. In this condition the maximum voltage error in the accelerating cavities respect to the average value is 0.4%. This value is fully acceptable from the beam dynamics point of view and in conclusion only one motorized tuner is necessary for each CCDTL module.

Measurements

Low power measurements

The measurements have been performed on the CERN CCDTL and ISTC CCDTL prototypes. The CERN prototype, entirely fabricated at CERN, consists on two half cells and one coupling cell [1].
In the table here below we summarize the results of the low level measurements for the CERN CCDTL prototype.

Frequency 0-mode	350.8185	MHz
Frequency $\pi/2$- mode	352.3547	MHz
Frequency π-mode	353.8653	MHz
Coupling k	0.86	%
Stop band	45	kHz
SWR = β	1.2384	#
Q_0	27281	#

Table 8 Results of the low level measurements for the CERN CCDTL prototype.

The frequency values in the table are the ones that were measured with the cavity under vacuum; at a pressure level of 10^{-8} mbar, a frequency shift of +67 kHz was observed for the $\pi/2$ mode and the stop-band changed from 20 to 45 kHz.
The ISTC CCDTL (RFNC-VNIITF Snezhinsk, Russia, and BINP Novosibirsk, Russia) prototype consists of 2 full accelerating cavities and one coupling cell. The structures have been designed to follow a certain velocity profile; hence the two cavities as well as the drift tubes have slightly different lengths. More details about the CERN CCDTL and ISTC CCDTL can be found in [2].
Table 9 summarizes the results of the low level measurements for the ISTC CCDTL prototype.

Frequency π /4-mode	350.8835	MHz
Frequency $\pi/2$- mode	352.1444	MHz
Frequency $3\pi/4$-mode	353.1497	MHz
Coupling k	0.90	%
Stop-band	62	kHz
Q_0	36700	#

Table 9 Results of the low level measurements for the ISTC CCDTL prototype.

The frequency values in the table are the ones that were measured with the cavity under vacuum; at a pressure level of $5 \cdot 10^{-7}$ mbar, a frequency shift of +84 kHz was observed for the $\pi/2$ mode. The Q_0 value is 82% of the theoretical value calculated with Superfish and meets the design specifications.

High power measurements

The power source consists of a LEP-type klystron (1 MW, CW), however fed by a power supply that is limited to 60 kV klystron voltage. The consequence is that the RF power out of the klystron is limited to about 350 kW.

For the test of the CERN prototype, a set of thermocouples was installed to monitor the temperature during the test. The vacuum in the prototype was of the order of 10-8 mbar. No strong multipacting levels were observed during the conditioning. Nominal field level requires 246 kW for 1.1 MV of effective voltage in each half cell. In the cavity, power in excess of 290 kW was measured at the pick-up. The temperature that initially was 27 deg. was stabilized at around 30 deg. with a minimum water flow of 5 l/min only in the drift tubes; the resonant frequency decreased by 7 kHz from cold to warm cavity condition.

After 2 more day of conditioning the CERN prototype was also tested at SPL duty cycle (50 Hz, 1ms): power in excess of 290 kW was measured at the pick-up in the accelerating cells.

In order to withstand the power dissipation of the cavity all the cooling channels were opened and a total flow of more that 30l/m was circulating inside the cavity[1]. The temperature of the drift tube holder, coupling iris and plunger tuner reached, respectively 58, 76 and 80 degrees. In particular the temperature rise in the coupling iris is due to the over-coupled matching between waveguide and cavity; the resonant frequency decreased by 128 kHz from cold to hot condition.

Finally, Figure 7 shows a plot of the power level in the cavity measured at the input directional coupler (forward power) and at the output pick-up in one of the half-tanks. This measurement was performed only for the CERN CCDTL prototype during the first high power test [4]. The two measured powers are identical over all the measurement range, indicating that no dark current was present during the test and hence that the voltage was still far from the breakdown limit.

[1] The measurement of the total water flow was limited by the flow-meter that saturates for value higher than 30 l/m

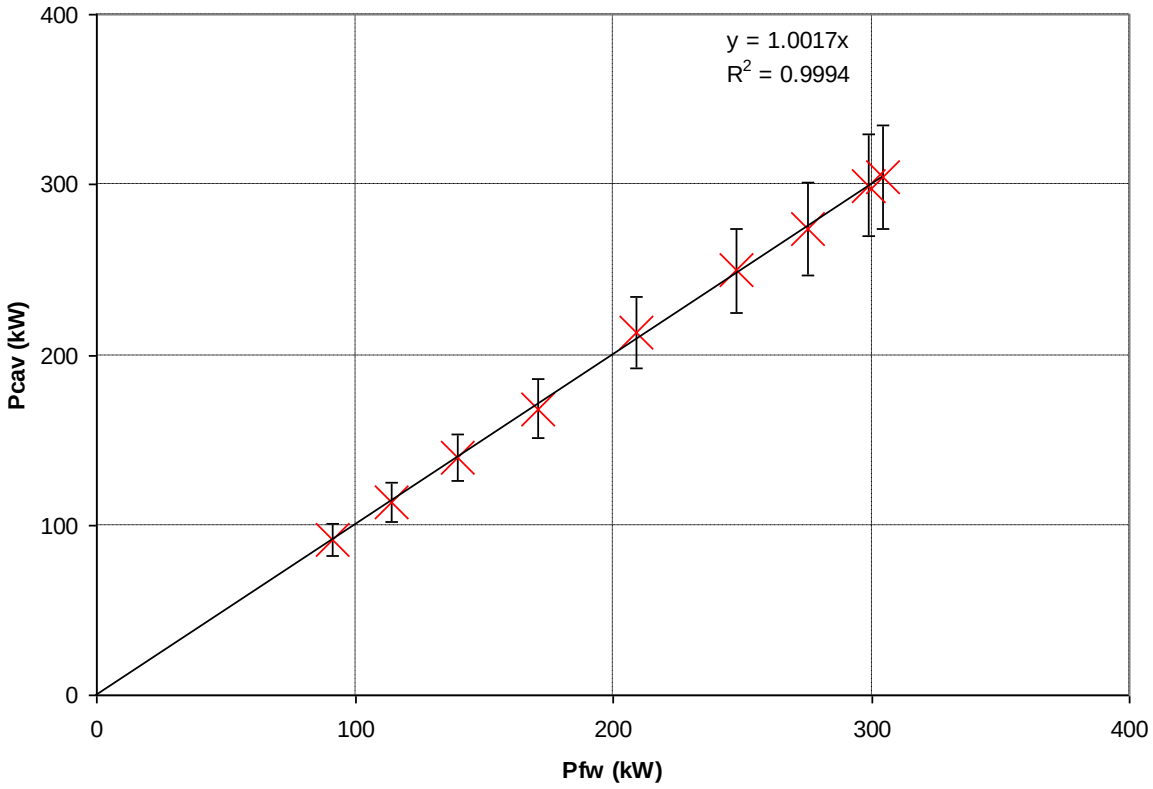

Figure 7 Power in the cavity vs. Power forward from the klystron.

Conditioning of the ISTC prototype lasted about a week. Minor multipactoring activity was observed at low power levels. Nominal field level requires 310 kW for 2.2 MV of effective voltage in each accelerating cavity. A power in excess of 330 kW at both Linac4 (0.1%) and SPL (5%) was measured in the cavity. The temperature on the cavity was monitored: at 5% duty cycle the temperature on the external part of the drift tube raised by 40 degrees, while tuners in the accelerating cell went up to 100 degrees. With the full water flow it was possible to stabilize the temperature with 330 kW power level at 11% duty cycle: (9 ms pulse period, 1 ms pulse length).

Mechanical Design

Two “hot” prototypes have been built to verify the electromagnetic and mechanical design of the CCDTL cavities. One short model was built at CERN. It consists of two half tanks, closed with copper plated lids at the position of the electric symmetry plane in the tanks, and one coupling cavity. The second model was built at VNIITF and BINP in Russia in the frame of ISTC contract 2875.

Each CCDTL cavity is assembled out of two copper-plated (30 um) stainless steel half-tanks. The half-tanks for the series production will be machined out of pre-shaped stainless steel “buckets”. For the prototypes the half-tanks were made of discs and cylinders, which were then electron-beam (EB) welded around the circumference with full penetration of the weld for the CERN prototype, whereas for the ISTC prototype discs and cylinders were TIG-welded before the final machining. The pre-shaped raw material (the “bucket-shape”) is around 10% more expensive but the savings in machining and welding time, together with the improved material properties of the half-tanks justify the additional initial expense. A smooth surface on the inside of the tank, instead of a machined welding, reduces risk of porosities

under the copper plating in the welding area and improves vacuum characteristics. Cooling channels are machined into the external part of the tanks.
Each half-tank contains one drift tube, which is machined out of solid copper and which is cooled via the supporting copper stem.

Vacuum tightness

Vacuum tightness and RF conductivity between separate parts (between: half-tanks, stem and tank, RF coupler port and cavity, cavity and coupling cells) are provided by Helicoflex type contacts. All vacuum flanges are (CERN) standard conflat flanges made of 316 LN steel, which are welded onto the port openings of the tanks. A critical area for the vacuum is the surface around the "racetrack-shaped" Helicoflex gasket, which connects the wave-guide with cavity. Since the port is not circular, the required surface roughness cannot be obtained via turning but the surface has to be rectified after machining. While turning produces a surface that has microgrooves in the direction of the gasket, any other type of machining produces microgrooves, which are not necessarily in the direction of the gasket and which carry a risk for vacuum leaks. To assess the risk of using a "racetrack-type" gasket a test set-up was constructed at VNIITF within an extension of ISTC contract 2875 that was paid by CERN. The test set-up consisted of two blank flanges with a rectified groove for the Helicoflex gaskets (Figure8).

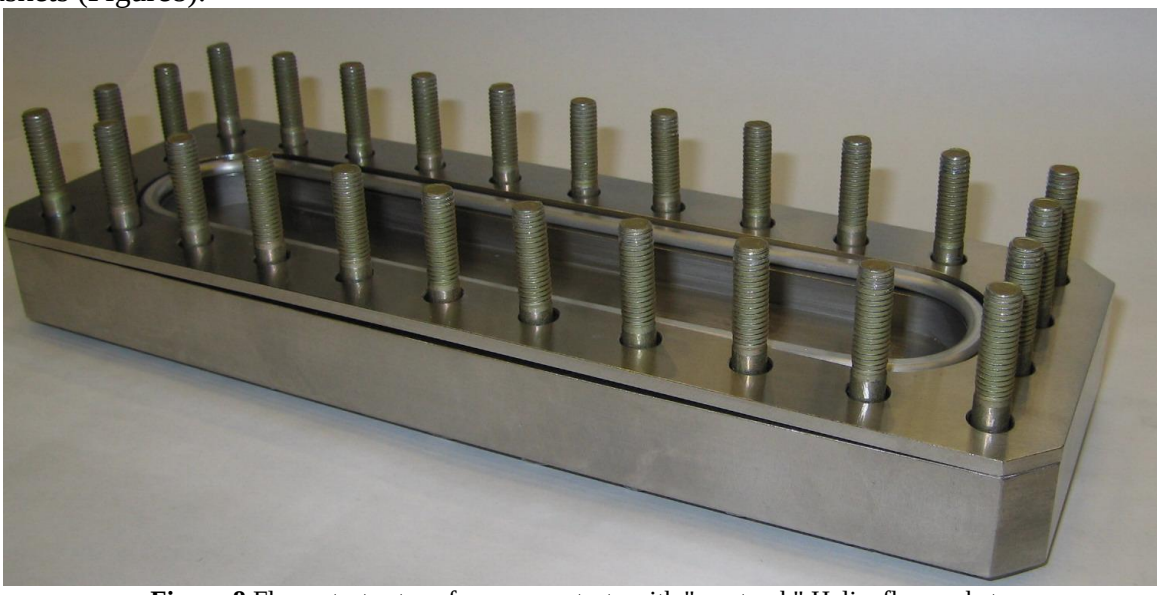

Figure 8 Flange test set-up for vacuum tests with "racetrack" Helicoflex gaskets

The test set-up was tested with HN-200 and HNV-200 Helicoflex gaskets using the machined or a copper plated surface. Out of 5 tests only one showed a leak, for a case where a copper plated surface was first used for an HNV gasket and then for an HN gasket. After re-plating the surface the leak disappeared. It was concluded to use a non-plated rectified surface together with an HN-200 type Helicoflex gasket to avoid any difficulties with surface imperfections.

Water cooling

The water cooling system is dimensioned for an operation at a 10% duty cycle for maximum water pressure of up to 16 bar. Water cooling channels are used in the outer tank shell, inside of the drift tubes, around the coupling cells and inside of the noses of the coupling cells. For the CCDTL production SERTO water fittings will connect the cooling channels of the tank

with the flexible cooling pipes on the outside. The fittings will be welded from the outside to the tank (Figure 9).

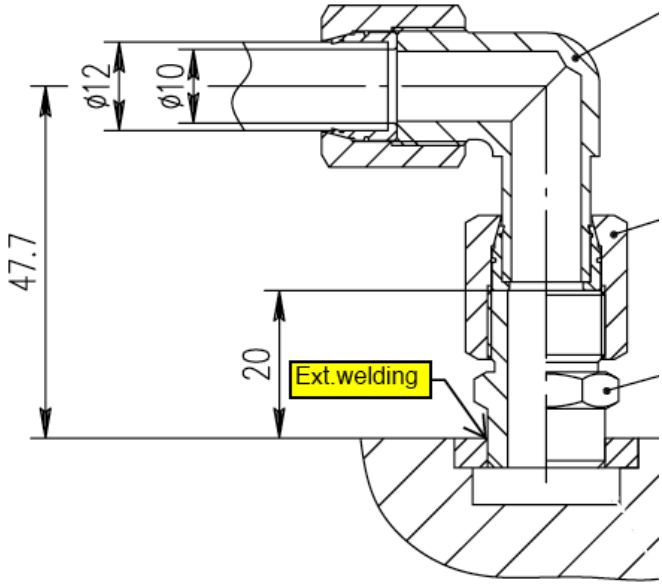

Figure 9 Welding of SERTO water connections to the tank.

The heating of the prototypes has been measured at CERN during the high-power tests of the VNIITF prototype. For this purpose thermocouples were used to monitor the temperature at various locations on the outside of the cavity. For a duty cycle of 2.5% the measured values were compared with simulations done at VNIITF and for most locations an excellent agreement was found (Table 10). Figure 10 shows the simulated temperature distribution in a half tank for a water flow of 0.5 m/s.

sensor	position	T_calc [°C]	T_meas [°C]
T1	outer surface of the 1st half-tank end wall	32.6	36
T2	outer surface of the 1st half-tank end wall	28.8	30
T3	outer surface of the 1st half-tank below the tuner port	40.7	59
T4	outer surface of 1st half-tank below the rf-pick-up	38.3	40
T5	outer surface of the 1st half-tank near the waveguide flange	30.3	31
T6	outer surface of the 1st half-tank below the eye-bolt holder	33.4	34
T7	outer surface of the 2nd half-tank near side pumping port	38.7	39
T8	out. surf. of the 2nd half-tank end wall above coupling iris	28.5	29
T9	out. surf. of the 2nd half-tank shell near stem connection	30.3	39
T10	**water inlet**	28.0	28
T11	**water outlet**	31.4	32

Table 10 Measured and simulated temperatures for various points on the surface of the tank for 2.5% duty cycle and 8 bar water pressure at the inlet (courtesy A. Tribendis, BINP).

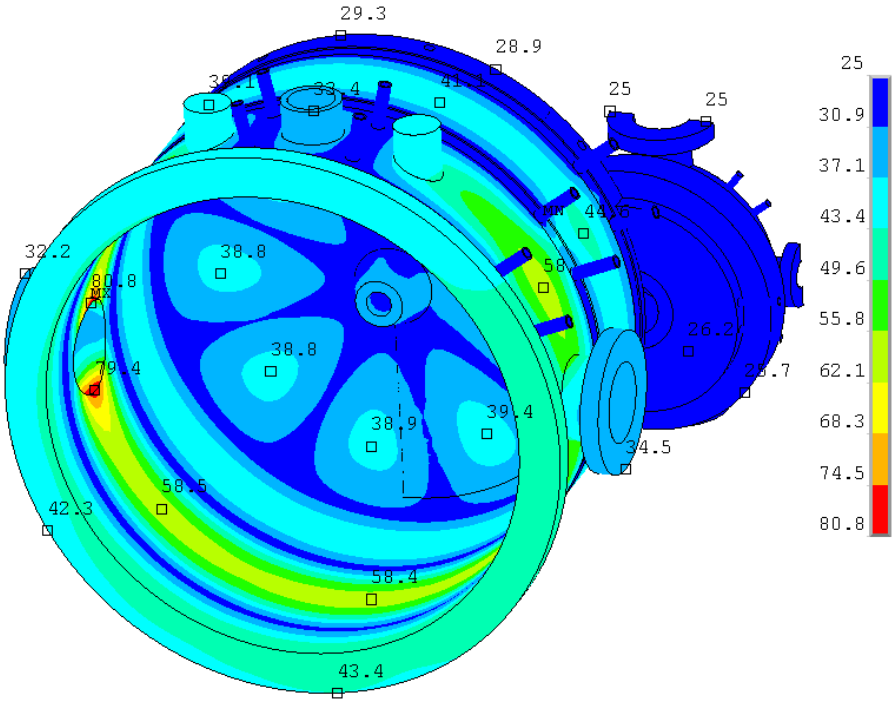

Figure 10 Simulated temperature map for half-tank with coupling cell for 0.5 m/s water flow (courtesy A.Tribendis).

Drift tube alignment

The drift tubes are electron beam welded to the stem and then fixed on a girder, which is fixed on top the tanks as shown in Figure 11. The alignment and fixing mechanism of the stem will be adapted from the CERN DTL design and it relies on the machining precision of the stem holder. This means that there is no possibility to change the alignment of the stems, other than re-machining the stem holder. Since there are no quadrupoles inside of the drift tubes, the required alignment precision for the stem is much less critical than for a DTL. The dismountable design was adapted because it allows an easy repair of the drift tubes in case of a fault. The alternative solution of welding the stems to the tanks, which was used for the prototypes, bears the risk of the stem changing its position due to inhomogeneous heating of the material.

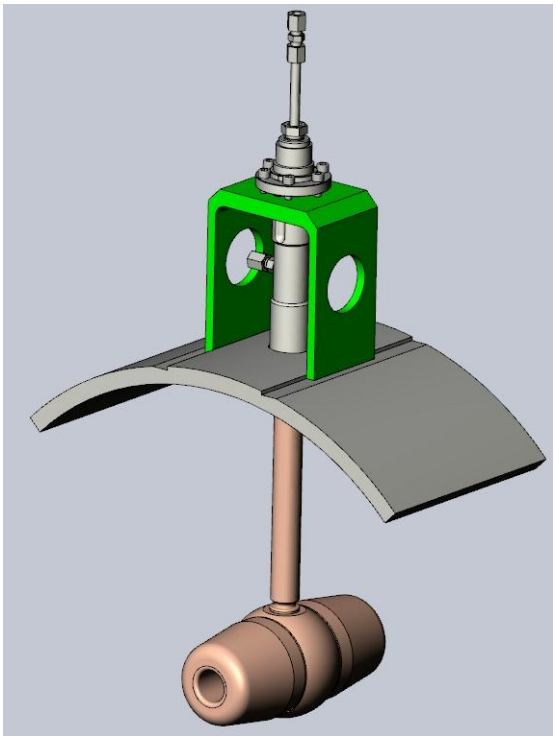

Figure 11 Dismountable drift tube and girder on top of the tank.

The vacuum tightness between stem and tank is given by a Helicoflex gasket, which is compressed by a defined force as shown in Figure 12.

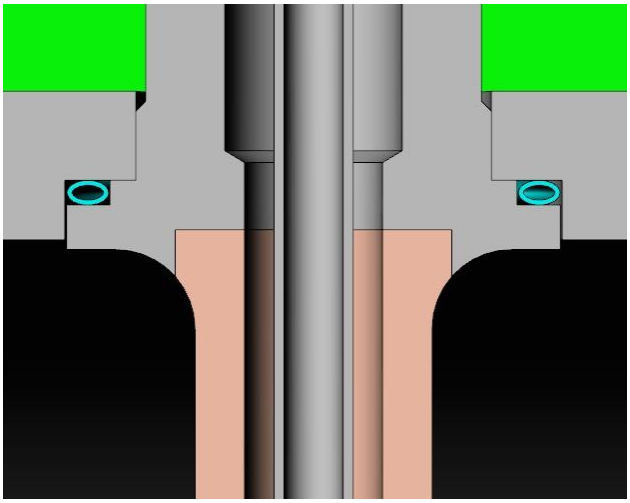

Figure 12 Helicoflex gasket between stem and tank.

The welding between the stem and the drift tube is a critical item because it defines the perpendicularity of the ensemble and thus the alignment precision of the drift tube in the tank. In the frame of the extension of ISTC contract 2875, BINP developed a technique that decouples the problem of perpendicularity from the welding process. As shown in Figure 13, the perpendicularity is given by the cylinder end surface, which is inserted into the drift tube. The surfaces, which are then connected by the welding, are slightly separated by a small gap, which is then closed with the weld. First tests at BINP have shown promising results and it is expected that this technique will be used for the series production.

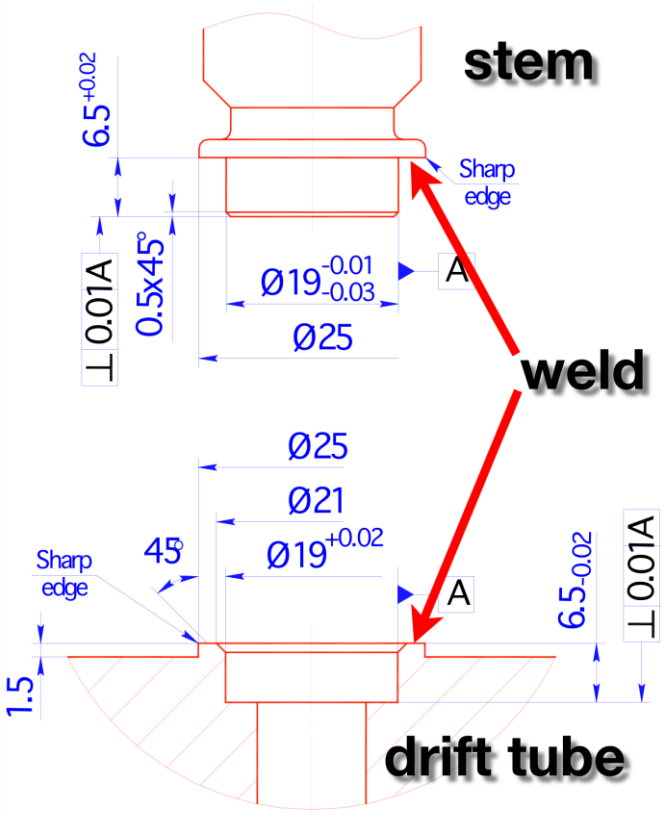

Figure 13 Welding of stem and drift tube.

Conclusions

A new CCDTL layout has been calculated with a starting energy of 50MeV. The final energy, after 21 cavities, is 102MeV. The basic guidelines for the calculation of the fundamental parameters have been given. In Table 11 we report the geometric parameters of the cavity geometry as that are used by the mechanical designers for the generation of the CCDTL layout.

Cavity #	Cavity length [mm]	Nose Cone [mm]	Gap [mm]	Drift Tube Length [mm]
1	695.0	45.4	64.3	205.7
2	712.7	47.5	67.2	207.9
3	731.9	50.4	70.4	210.0
4	749.1	52.2	73.4	212.1
5	768.8	55.1	76.8	214.1
6	785.4	56.7	79.9	216.1
7	804.8	59.6	83.3	217.9
8	821.3	61.1	86.5	219.7
9	840.7	64.0	90.0	221.4
10	856.2	65.2	93.2	223.1
11	875.9	68.3	96.8	224.6
12	890.9	69.2	100.0	226.3
13	910.1	72.3	103.5	227.5
14	924.2	73.0	106.7	229.1
15	942.6	75.9	110.2	230.2
16	956.3	76.6	113.3	231.6
17	974.1	79.5	116.7	232.6
18	986.8	79.9	119.7	233.9
19	1004.5	82.7	123.1	234.8
20	1015.9	82.9	125.9	236.1
21	1033.4	85.9	129.3	236.8

Table 11 Variable geometry parameters of the CCDTL section.

References

[1] M. Vretenar *et al.* Development of a 352 MHz Cell-Coupled Drift Tube Linac Prototype, Proc. LINAC04 Lübeck
[2] M. Pasini *et al.*, CCDTL prototypes: test results, CARE/HIPPI Document-2007-036
[3] M. Pasini, CCDTL design update for Linac4, CARE/HIPPI Document-2005-009
[4] M. Pasini *et al.*, CCDTL prototype: status report, CARE/HIPPI Document-2006-021

Acknowledgements

We acknowledge the support of the European Community-Research Infrastructure Activity under the FP6 “Structuring the European Research Area” programme (CARE, contract number RII3-CT-2003-506395)

Appendix A

A typical CDTfish control file follows (Figure 14):

```
; CDTfish control file

Title
2-drift-tube CCDTL cavity
352.2-MHz half cell with 2-cm-long bore tube
Equal face angles on drift tubes
ENDTitle

PARTICLE          H-
TEMPerature       25

FULL_cavity
FILEname_prefix              cav1
SEQuence_number                 1
FREQuency                  351.56
BETA                       0.3166
DIAMeter                       52
GAP_Length                    6.7
E0_Normalization                4
NUMBER_of_gaps                  3
EQUATOR_flat               61.500
INNER_CORNer_radius           1.5
OUTER_NOSE_radius             0.7
INNER_NOSE_radius             0.2
FLAT_length                   0.3
CONE_angle                     20
SEPTUM_thickness              -2.0
BORE_radius                   1.4
LEFT_BEAM_tube                  8
RIGHT_BEAM_tube                 8
DT_DIAMeter                   9.5
DT_CORNer_radius             0.25
DT_OUTER_NOSE_radius          1.2
DT_INNER_NOSE_radius          0.2
DT_FLAT_length                0.3
DT_STEM_Diameter              2.4
DT_STEM_Count                   1
DT_FACE_angle                 0.0
DT_OUTER_FACE_angle            75
DT_INNER_FACE_angle            75
RING_TYPE                     0.0
RING_DY                       0.0
RING_Width                    0.0
RING_Angle                    0.0
RING_Effect                   0.0
RING_THickness                0.0
DELTA_frequency              0.05
```

```
MESH_size                0.05
INCrement                   2
START                       5

; Start codes for CDTfish:
; 1 No tuning
; 2 Adjust diameter and move gaps for S = 0
; 3 Adjust gap(s) and move gaps for S = 0
; 4 Adjust diameter, gap centers fixed
; 5 Adjust gap(s), gap centers fixed
;  (When S = 0, geometric and electrical centers coincide.)
; Ring_Type codes for CDTfish:
; 0 No tuning ring
; 1 Equator ring of a given thickness.
; 2 Equator ring of a given frequency effect.
; 3 Wall rings of a given thickness.
; 4 Wall rings of a given frequency effect.

EndFile
```

Figure 14 Control file for the first cavity of CCDTL structure.

Appendix B

Summary tables of the CCDTL Excel file generation.

N. Cav #	E0 [MV/m]	βg #	βg SF #	βini #	V1 [MV]	TTFg1 [#]	ϕgap1 [deg]	ΔW1 [MeV]	E1 [MeV]	β end g1 #
1	**4**	**0.3172**	**0.3166**	0.313891	0.8161906	0.86609	**-21.6**	0.657254	50.7	0.315792
2	**4**	**0.3233**	**0.3227**	0.320161	0.8323554	0.86113	**-21.4**	0.667349	52.9	0.32204
3	**4**	**0.3294**	**0.3288**	0.326352	0.8495743	0.856216	**-21.3**	0.67773	55.1	0.328212
4	**4.1**	**0.3355**	**0.3349**	0.332464	0.8869487	0.850266	**-21.3**	0.702628	57.4	0.334345
5	**4.1**	**0.3417**	**0.3411**	0.338644	0.9047699	0.844818	**-21.3**	0.712153	59.7	0.340502
6	**4.1**	**0.3478**	**0.3472**	0.344738	0.9203747	0.838977	**-21.3**	0.719427	62.1	0.346569
7	**4.2**	**0.3538**	**0.3532**	0.350753	0.9607388	0.832087	**-21.2**	0.745317	64.5	0.352604
8	**4.2**	**0.3598**	**0.3591**	0.356819	0.9765184	0.82671	**-21.2**	0.752663	66.9	0.358643
9	**4.2**	**0.3658**	**0.3651**	0.362798	0.9942417	0.819483	**-21.1**	0.760137	69.4	0.364596
10	**4.3**	**0.3716**	**0.3709**	0.368691	1.033059	0.813932	**-21**	0.784992	72.0	0.370505
11	**4.3**	**0.3775**	**0.3768**	0.374634	1.051613	0.806761	**-21**	0.79205	74.6	0.376421
12	**4.3**	**0.3833**	**0.3826**	0.380477	1.065984	0.800851	**-21**	0.796992	77.2	0.382235
13	**4.23**	**0.3889**	**0.3882**	0.386231	1.066565	0.792832	**-20.9**	0.78997	79.8	0.387934
14	**4.23**	**0.3945**	**0.3938**	0.391794	1.079987	0.787301	**-20.9**	0.794331	82.4	0.39347
15	**4.23**	**0.3999**	**0.3992**	0.397276	1.097122	0.779841	**-20.9**	0.799287	85.0	0.398926
16	**4.16**	**0.4052**	**0.4045**	0.402664	1.092008	0.773972	**-20.9**	0.789574	87.7	0.40426
17	**4.16**	**0.4103**	**0.4096**	0.407883	1.108271	0.76638	**-20.7**	0.794526	90.3	0.409457
18	**4.16**	**0.4154**	**0.4146**	0.413016	1.120129	0.760664	**-20.7**	0.797037	92.9	0.414563
19	**4.1**	**0.4205**	**0.4197**	0.418071	1.120065	0.752926	**-20.7**	0.788884	95.5	0.419572
20	**4.1**	**0.4253**	**0.4245**	0.42297	1.130419	0.747851	**-20.7**	0.79081	98.1	0.424447
21	**4.1**	**0.4301**	**0.4293**	0.427797	1.146506	0.74039	**-20.7**	0.794062	100.7	0.429252

V2 [MV]	TTFg2 [#]	ϕgap2 [deg]	ΔW2 [MeV]	E2 [MeV]	β end g2 #	V3 [MV]	TTFg3 [#]	ϕgap3 [deg]	ΔW3 [MeV]	E3 [MeV]	β end g3 #
1.067897	0.867624	-19.9945697	0.870686	51.5	0.31828596	0.8161264	0.86812	-21.22285	0.660445	**52.2**	0.320161
1.087417	0.863181	-19.99152322	0.882078	53.7	0.32450173	0.8324769	0.862851	-21.32471	0.669124	**54.4**	0.326352
1.105231	0.85718	-19.99743492	0.890262	56.0	0.33063419	0.8494298	0.857933	-21.34125	0.678783	**56.7**	0.332464
1.153614	0.852355	-20.0559602	0.92366	58.3	0.33679425	0.8867946	0.8526	-21.43939	0.703764	**59.0**	0.338644
1.172082	0.8459	-20.03360221	0.931473	60.6	0.34291115	0.9046357	0.845492	-21.30511	0.712591	**61.3**	0.344738
1.193983	0.841029	-20.02132855	0.943487	63.0	0.34894962	0.9203582	0.840292	-21.20736	0.720995	**63.7**	0.350753
1.241058	0.833017	-19.97929052	0.971603	65.4	0.35499663	0.9604818	0.833508	-21.19279	0.746426	**66.2**	0.356819
1.263246	0.827426	-20.0385871	0.981966	67.9	0.36100278	0.9762832	0.827743	-21.23803	0.753228	**68.7**	0.362798
1.281188	0.821107	-19.91159378	0.989104	70.4	0.3669175	0.9942097	0.82082	-21.00803	0.761823	**71.2**	0.368691
1.334459	0.815483	-19.93576935	1.023017	73.0	0.3728493	1.033017	0.814674	-21.14202	0.784925	**73.8**	0.374634
1.351322	0.808047	-19.96821539	1.026287	75.6	0.37871875	1.051429	0.807272	-21.12673	0.791738	**76.4**	0.380477
1.375274	0.801521	-19.9967105	1.035855	78.2	0.38450109	1.066294	0.80128	-21.12126	0.797001	**79.0**	0.386231
1.367839	0.794031	-20.00384319	1.020581	80.8	0.39011787	1.066499	0.793611	-21.12769	0.789491	**81.6**	0.391794
1.391162	0.787698	-19.95734617	1.030008	83.4	0.395626	1.080127	0.787461	-20.98195	0.79416	**84.2**	0.397276
1.405715	0.780047	-20.0212343	1.030256	86.1	0.40103743	1.097125	0.78081	-21.04227	0.799521	**86.9**	0.402664
1.40369	0.774957	-20.06281792	1.021789	88.7	0.40631062	1.091703	0.774557	-21.04685	0.789175	**89.5**	0.407883
1.415952	0.767638	-19.958705	1.021656	91.3	0.41146614	1.108091	0.766821	-20.97899	0.793382	**92.1**	0.413016
1.437525	0.761428	-19.97305053	1.028737	93.9	0.41654613	1.11995	0.761271	-20.96359	0.796151	**94.7**	0.418071
1.429096	0.754166	-19.90380268	1.013395	96.5	0.42148808	1.12	0.753432	-20.74773	0.78912	**97.3**	0.42297
1.450135	0.748721	-19.97643626	1.020421	99.1	0.42633988	1.130438	0.74827	-20.8545	0.790458	**99.9**	0.427797
1.459444	0.741442	-19.98865773	1.016908	101.7	0.43110333	1.146611	0.740695	-20.8265	0.793798	**102.5**	0.432539

power [kw]	gap [cm]	s [cm]	Beam load [kw]	Tot power/cav [kw]	tot power [kw]	beam loading ratio %
148.451	6.429376	**2**	87.53541344	265.6766134	265.67661	37.09341235
150.052	6.724844	2.469684	88.7420895	268.8044895	534.4811	37.16259883
151.323	7.035906	3.092531	89.87100502	271.458605	805.93971	37.26087844
160.91	7.344467	3.513906	93.20207414	286.2940741	286.29407	36.67754649
162.397	7.67591	4.162952	94.24864788	289.1250479	575.41912	36.72325974
164.615	7.990337	4.525065	95.35637131	292.8943713	868.31349	36.67956623
174.299	8.328489	5.184424	98.53383648	307.6926365	307.69264	36.11509441
176.613	8.652874	5.560784	99.51423969	311.4498397	619.14248	36.03926936
178.331	9	6.225387	100.4425613	314.4397613	933.58224	36.03016039
189.498	9.320059	6.541078	103.7173535	331.1149535	331.11495	35.37241562
191.225	9.676472	7.268758	104.4030147	333.8730147	664.98797	35.31567021
194.018	10	7.532978	105.1939531	338.0155531	1003.0035	35.15700225
189.329	10.35268	8.270543	104.0016787	331.1964787	331.19648	35.45543861
192.1	10.67157	8.478665	104.7399691	335.2599691	666.45645	35.28499528
193.742	11.01716	9.175464	105.1625978	337.6529978	1004.1094	35.18266315
189.877	11.32817	9.410768	104.0215017	331.8739017	331.8739	35.39368222
191.39	11.665	10.10548	104.3825347	334.0505347	665.92444	35.29149007
193.951	11.96566	10.27484	104.8770197	337.6182197	1003.5427	35.09611308
189.914	12.3125	10.95981	103.65598	331.55278	331.55278	35.30878056
192.445	12.59111	11.06212	104.0675409	335.0015409	666.55432	35.09718025
193.79	12.92625	11.80543	104.190729	336.738729	1003.293	34.96559303

equator flat [cm]	length/cav [m]	tot length [m]	kilp scaled [#]	β center []	Clenght+Septum	ZTT
61.500119	0.94500119	0.94500119	1.74502	0.31704211	69.50011902	53.14898306
63.2678822	0.962671982	1.907673173	1.72429	0.32327405	71.26788224	52.67485984
65.1888089	0.981892774	2.889565947	1.70031	0.32942636	73.18880888	52.14705673
66.9082629	0.999093567	3.888659514	1.72632	0.33557252	74.90826291	51.57506114
68.8766682	1.018807159	4.907466672	1.70519	0.34170963	76.87666816	50.88483762
70.5368603	1.035407951	5.942874623	1.69395	0.34776221	78.53686031	50.27582564
72.4730178	1.054765943	6.997640566	1.716	0.35380339	80.4730178	49.45024483
74.1261778	1.071303935	8.068944501	1.70609	0.35982567	82.12617776	48.79537767
76.0675799	1.090681927	9.159626428	1.69005	0.36575965	84.06757992	48.00038814
77.6175099	1.10616432	10.26579075	1.72431	0.37167975	85.61750986	47.30582942
79.6007093	1.125929512	11.39172026	1.70835	0.37757257	87.60070928	46.43484706
81.0991687	1.140911905	12.53263217	1.70578	0.38337046	89.09916872	45.68361766
83.0284124	1.160128698	13.69276086	1.66334	0.38902844	91.02841242	44.77440557
84.4282144	1.17415549	14.86691635	1.66318	0.39455014	92.42821435	44.04474264
86.2741323	1.192596683	16.05951304	1.65082	0.39998401	94.27413231	43.18449137
87.6372755	1.206335077	17.26584811	1.62325	0.40528732	95.63727548	42.50459144
89.4172714	1.22410787	18.48995598	1.61189	0.41046348	97.41727143	41.62534574
90.6719102	1.236820663	19.72677665	1.61405	0.41555643	98.67191022	40.93542472
92.4421514	1.254493457	20.9812701	1.58007	0.42053186	100.4421514	40.06792787
93.5659019	1.265877851	22.24714795	1.58457	0.42539514	101.5659019	39.44616246
95.3306552	1.283392244	23.5305402	1.57304	0.43017925	103.3306552	38.59956305